


## Mesenchymal Stem Cells Reduce Corneal Fibrosis and Inflammation via Extracellular Vesicle-Mediated Delivery of miRNA

GOLNAR SHOJAATI,<sup>a,b</sup> IRONA KHANDAKER,<sup>a</sup> MARTHA L. FUNDERBURGH,<sup>a</sup> MARY M. MANN,<sup>a</sup> ROHAN BASU,<sup>a</sup> DONNA B. STOLZ,<sup>a</sup> MOIRA L. GEARY,<sup>a</sup> AURÉLIE DOS SANTOS,<sup>c</sup> SOPHIE X. DENG,<sup>c</sup> JAMES L. FUNDERBURGH <sup>a</sup>

**Key Words.** Mesenchymal stem cells • Extracellular vesicles • Exosomes • Regeneration • Cornea • MicroRNA

<sup>a</sup>Department of Ophthalmology, University of Pittsburgh, Pittsburgh, Pennsylvania, USA; <sup>b</sup>Kantonsspital Winterthur, Zurich, Switzerland; <sup>c</sup>Stein Eye Institute, University of California Los Angeles, Los Angeles, California, USA

Correspondence: James L. Funderburgh, Ph.D., Department of Ophthalmology, 203 Lothrop Street, Pittsburgh, Pennsylvania 15213, USA. Telephone: 412-647-3853; e-mail: jlfunder@pitt.edu

Received December 31, 2018; accepted for publication May 25, 2019; first published July 10, 2019.

<http://dx.doi.org/10.1002/sctm.18-0297>

This is an open access article under the terms of the Creative Commons Attribution-NonCommercial-NoDerivs License, which permits use and distribution in any medium, provided the original work is properly cited, the use is non-commercial and no modifications or adaptations are made.

### ABSTRACT

Mesenchymal stem cells from corneal stromal stem cells (CSSC) prevent fibrotic scarring and stimulate regeneration of transparent stromal tissue after corneal wounding in mice. These effects rely on the ability of CSSC to block neutrophil infiltration into the damaged cornea. The current study investigated the hypothesis that tissue regeneration by CSSC is mediated by secreted extracellular vesicles (EVs). CSSC produced EVs 130–150 nm in diameter with surface proteins that include CD63, CD81, and CD9. EVs from CSSC reduced visual scarring in murine corneal wounds as effectively as did live cells, but EVs from human embryonic kidney (HEK)293T cells had no regenerative properties. CSSC EV treatment of wounds decreased expression of fibrotic genes *Col3a1* and *Acta2*, blocked neutrophil infiltration, and restored normal tissue morphology. CSSC EVs labeled with carboxyfluorescein succinimidyl ester dye, rapidly fused with corneal epithelial and stromal cells in culture, transferring microRNA (miRNA) to the target cells. Knockdown of mRNA for Alix, a component of the endosomal sorting complex required for transport, using siRNA, resulted in an 85% reduction of miRNA in the secreted EVs. The EVs with reduced miRNA were ineffective at blocking corneal scarring. Furthermore, CSSC with reduced Alix expression also lost their regenerative function, suggesting EVs as an obligate component in the delivery of miRNA. The results of these studies support an essential role for extracellular vesicles in the process by which CSSC cells block scarring and initiate regeneration of transparent corneal tissue after wounding. EVs appear to serve as a delivery vehicle for miRNA, which affects the regenerative action. *STEM CELLS TRANSLATIONAL MEDICINE* 2019;8:1192–1201

### SIGNIFICANCE STATEMENT

Recent advances in stem cell therapy have demonstrated the potential to restore vision to individuals suffering from corneal scarring. This study demonstrates that the regenerative potential of stem cells from human cornea can be duplicated by delivery of microRNA to ocular tissues by extracellular vesicles. The results open an important avenue for elucidation of the molecular mechanism governing the regenerative process. This information can potentially lead to rapid and inexpensive means of treating corneal blindness for millions of individuals who have no further options for treatment.

### INTRODUCTION

Mesenchymal stem cells (MSCs) are the subject of intense research due to their high regenerative potential and broad spectrum of applicability in experimental and clinical settings [1]. MSCs can be isolated from multiple tissues, including adipose tissue and bone marrow. Our previous work has shown that human corneal stroma contains a population of cells (human corneal stem cells, CSSC), which exhibit properties of

MSCs and differentiate to corneal keratocytes [2–9]. These cells also block deposition of opaque scar tissue in a corneal wound healing model and elicit regeneration of normal, transparent stromal extracellular matrix [7, 8, 10–12]. An important aspect of tissue regeneration effected by MSCs depends on their modification of tissue immune response by secretion of soluble factors to their environment [13–16]. We found that CSSC suppressed early neutrophil infiltration in response to corneal trauma and

that the presence of neutrophils was essential to the development of opaque scar tissue [7]. This immunomodulatory effect is consistent with that demonstrated by MSCs from other sources [17, 18]; however, the mechanism by which immunomodulatory factors are delivered to neutrophils, and the possibility that CSSC elicit additional effects on cells of the host tissue needs to be better elucidated.

CSSC-induced corneal regeneration does not require direct interaction between stem cells and the host cells [10], an effect that is consistent with the paracrine action of MSCs from other sources in eliciting regenerative responses [14]. A number of soluble factors have been identified in the secretome of MSCs as active in the regenerative process [19]; however, recent reports have demonstrated that MSCs can communicate with target cells via secretion of extracellular vesicles (EVs) released by the MSCs. EVs fuse with remote cells delivering a cargo of protein and RNA that can modify the phenotype of the target cells [14, 20–22]. Involvement of EVs has been implicated in regenerative effects of MSCs in a wide variety of tissues including skin, muscle, neural tissues, lung, vascular tissue, bone, and cartilage [21, 23–29]. MicroRNA (miRNA) has been frequently cited as an important mediator of the biological effects of MSC-secreted EVs [1, 23, 24, 30, 31].

The current study examined a potential role for EVs in the regeneration of damaged cornea by CSSC. We find that CSSC produce EVs, which effectively deliver regenerative phenotype to the tissue in an miRNA-dependent manner.

## MATERIALS AND METHODS

### Isolation of CSSC

Human corneo-scleral rims, approved for research purposes, from de-identified donors younger than 60 years, were obtained from the Center for Organ Recovery and Education, Pittsburgh, PA ([www.core.org](http://www.core.org)). Tissue was used within 5 days of enucleation. Research followed the tenets of the Declaration of Helsinki and was approved by the University of Pittsburgh Institutional Review Board and Committee for Oversight of Research and Clinical Training Involving Decedents, Protocol #161. CSSCs were obtained from dissected limbal tissue using collagenase digestion as previously described [10]. Cells were seeded into a 25 cm<sup>2</sup> tissue culture flask in stem cell growth medium (JMH) with 2% (vol/vol) pooled human serum (JMH) as previously described [10]. Culture medium was changed at 3-day intervals and cells were passaged by brief digestion with recombinant trypsin (TrypLE Express, Thermo Fisher Scientific, MA) when 80% confluent into a 175-cm<sup>2</sup> T-flask and cryopreserved at passage 1. Cells, unless otherwise noted, were used from a single donor (line HC461). They were demonstrated to be a homogeneous population using flow cytometry with cell surface markers conventionally used to identify bone marrow MSC, CD90, CD73, and CD105 (Supporting Information Fig. S1). Cells were used at passage 3.

### Mouse Corneal Wound Model

This study was carried out in accordance with the recommendations in the Guide for the Care and Use of Laboratory Animals of the National Institutes of Health and The Association for Research in Vision and Ophthalmology Statement for the Use of Animals in Ophthalmic and Vision Research. It was

approved by the Institutional Animal Care and Use Committee of the University of Pittsburgh, Protocol #15025426. Procedures were adapted to minimize pain and suffering in the animal subjects. Female C57/BL6 mice, 7–8 weeks of age, were obtained from Charles River Laboratories International, Inc., housed in an AALAC-approved ABSL2 facility, and provided an unrestricted standard diet. Groups of six mice were anesthetized by intraperitoneal injection of ketamine (50 mg/kg) and xylazine (5 mg/kg). Our previous study and power analysis determined that at least six eyes were required for statistical significance in visible scar analysis and that 2 weeks provided an appropriate time point for analysis of gene expression and fibrosis [10, 32]. One drop of proparacaine hydrochloride (0.5%) was added to each eye before debridement for topical anesthesia. Debridement procedures were done as previously described [10]. Corneal epithelial debridement was performed by passing an AlgerBrush II (The Alger Company, TX) over the central 2 mm of the mouse cornea. Once the epithelium was removed, a second application of the AlgerBrush II was used, this time applying more pressure to remove the basement membrane and 10–15  $\mu$ m of anterior stromal tissue. Immediately after the procedure, mice received ketoprofen (3 mg/kg) for analgesia. Both eyes received the same wounding and treatment. CSSC, 10<sup>6</sup> cells per milliliter in phosphate-buffered saline (PBS), or purified EVs (10<sup>10</sup> particles per milliliter, 0.5 mg/ml protein) were mixed 1:1 with human fibrinogen (Sigma Chemical, St. Louis, MO), 75 mg/ml in PBS and maintained on ice. After wounding, 0.5  $\mu$ l of thrombin (100 U/ml, Sigma) was added to the wound bed, followed immediately by 1  $\mu$ l of fibrinogen (with or without CSSC or EV). Fibrin gelled within 1 minute, and a second round of thrombin and fibrinogen was applied. The wound was treated with a drop of gentamicin ophthalmic solution (0.3%). The corneal epithelium reformed over the wound within 24 hours.

### Assessment of Scarring

Two weeks after corneal debridement, all eyes were collected and the whole globes were imaged using a dissecting microscope with indirect illumination [11]. Scar area was determined by two independent observers from these images, with identity of the samples masked, using the Fiji open-source image analysis software package (<https://fiji.sc/>). Statistical analyses of results were performed with Prism 7 (GraphPad Prism, CA) using *t* tests or Dunn's test as noted in the text. In some experiments, scar intensity was scored by three independent observers masked as to treatment of the eyes using a standard five point scoring system as follows: score: 0 = no opacity, completely transparent cornea; 1 = slight haze, iris and lens are clearly visible; 2 = moderate opacity, iris and lens still well defined; 3 = severe opacity, details of iris and lens are obscured; 4 = complete opacity, iris and lens are not distinguishable. Average scores were determined and statistical analyses were performed as describe above.

Corneal gene expression was carried out as previously described [7, 10, 11]. Six corneas per group were dissected and pooled in 700  $\mu$ l RLT extraction reagent (Qiagen, Germantown, MD) then disrupted with MagNA Lyser green beads using six cycles at 6,000 RPM with intermittent cooling in a MagNA Lyser Instrument (Roche, Indianapolis, IN). The extracts were further processed using Qia-shredder (Qiagen), and RNA was isolated by Qiagen RNeasy Minikit. Five hundred nanograms total RNA was transcribed to cDNA using SuperScript III (Thermo

Fisher Scientific, MA) as previously described [10]. cDNA and target primers were combined with SYBR Green Real-Time Master Mix (Thermo Fisher Scientific, MA) and real-time polymerase chain reaction (PCR) run and data analyzed using the StepOnePlus Real-Time PCR System (Thermo Fisher Scientific, MA) [10]. Relative mRNA abundance was compared by delta-delta Ct method using 18S RNA as an endogenous control [10].

### siRNA Knockdown of Alix Expression

CSSC ( $10^6$  cells) cultured overnight in a 100 mm dish were transfected with Alix(PDCD6IP) siRNA (Silencer Select, Thermo Fisher Scientific, MA) or a scrambled control siRNA, 42 nM in 9 ml JMH medium using Viromer Blue transfection agent (OriGene Technologies, MD) according to the manufacturer's instructions. Cells were cultured at 37°C for 72 hours in JMH medium and EVs were prepared as described below. CSSC were lysed in 1× SDS sample buffer and subjected to immunoblotting using antibody to Alix protein (Clone 3A9, Thermo Fisher Scientific, MA) using methodology described previously [7].

### Neutrophil Myeloperoxidase Assay

Assessment of neutrophil infiltration was estimated as previously described by measurement of myeloperoxidase in corneas 24 hours after wounding [33]. Mouse corneas were excised and dissected 24 hours after wounding, removing all residual iris and scleral tissues, and each cornea was incised radially. Individual corneas were placed in 0.3 ml tissue extraction buffer (Thermo Fisher Scientific, MA) containing 1:100 protease inhibitor cocktail (Sigma-Aldrich, P8340) and disrupted by sonication in 4× 30-second bursts, with cooling on ice between bursts. The homogenate was centrifuged for 15 minutes at 14,000g at 4°C. Myeloperoxidase (MPO) activity was determined in 1:20 dilution of the homogenate using a fluorometric immunoassay (R&D Systems, DY3667, MN) according to the manufacturer. Each sample was analyzed in triplicate and MPO was calculated from a standard curve.

### EV Isolation and Analysis

Human CSSC at passage 3 were cultured in JMH medium as previously described [7]. Isolation of the EVs followed guidelines presented in the 2018 MISEV [34]. At confluence, cells were rinsed and cell growth medium was replaced with the same medium containing 2% human serum, which had been cleared of particulate material by 18 hours centrifugation at 100,000g. After 72 hours, conditioned media were collected, passed through 0.22 µm filters and concentrated 20× by centrifugation at 4,000g in Amicon Ultra 100k cutoff ultrafilters. EVs were precipitated by polymer exclusion using Total Exosome Purification Reagent (Invitrogen, 4478359) and the pellet was resuspended overnight in PBS with gentle shaking at 4°C. Samples were centrifuged at 4°C for 1 hour at 10,000g and then EVs were recovered from the supernatant by centrifugation at 100,000g for 3 hours. The pellet was rinsed and resuspended by shaking in PBS overnight, EVs were pelleted by a second cycle at 3 hours at 100,000g, and the final solution in PBS was filtered through 0.22 µm filters. Protein concentration was estimated by UV absorbance at 260 nm and 280 nm. Particle size and concentration were determined by Tunable Resistive Pulse Sensing (TRPS) using a qNano Gold Instrument (Izon Science, MA). Calnexin and CD63 were examined by immunoblotting

using Anti-CD63 (ThermoFisher #10628D) and anti-calnexin (Clone AF18, Thermo Fisher Scientific, MA).

### Transmission Electron Microscopy

Conditioned culture medium, after 0.22 µm filtration was centrifuged using a Beckman-Coulter Airfuge at 100,000g for 45 minutes. Pellet material was transferred to a copper grid coated with 0.125% Formvar in chloroform. The grids were stained with 1% vol/vol uranyl acetate in ddH<sub>2</sub>O and the samples were examined immediately, using a JEOL 1011 transmission electron microscope.

### Flow Cytometric Analysis of EVs

Anti-CD63 magnetic beads (Dynabeads 10606D, Thermo Fisher Scientific; 15 µl containing  $1.5 \times 10^5$  beads) were incubated with samples containing  $10^7$ – $10^8$  EV particles in a volume of 50 µl bovine serum albumin (BSA), 1 mg/ml in PBS (BSA-PBS) overnight at 4°C with gentle shaking. Preliminary experiments indicated that these conditions captured >85% of EV particles measured by TRPS or fluorescent-labeled EVs (data not shown). The samples were rinsed 3× in PBS by magnetic capture and then incubated in a volume of 50 µl PBS-BSA containing fluorescent antibodies to one or combinations of the following markers: CD81, CD9, CD29, CD13, CD90, CD36, HLAG, HLA-DR, CD34, CD146, CD107a, CD274, CD166, CD44, CD74, or CD59 (BioLegend, CA) for 2 hours at room temperature. After 3× rinsing in PBS the beads were analyzed by flow cytometry using a BD FACS Aria III instrument. A majority of beads with mean fluorescence greater than that of the isotype control antibody was considered indication of presence of the targeted protein (Supporting Information Fig. S1). Triplicate analyses were carried out for all samples.

### Carboxyfluorescein Succinimidyl Ester Labeling and Loading of EVs with miRNA

Filtered conditioned media from CSSC concentrated 20× (as described above) was incubated with carboxyfluorescein succinimidyl ester (CFSE, Thermo Fisher Scientific, V12883) 20 µM, 2 hours at 37°C. EVs were purified from this medium as described above. CFSE-labeled EVs (47 µg protein in 100 µl) were loaded with nonmammalian miR159a (12 µg RNA) by incubation in PBS with 0.1 M CaCl<sub>2</sub> on ice for 30 minutes followed by 42°C for 5 minutes and returned to 4°C as previously described [35]. EVs were recovered by pelleting as above.

### Transfer of EVs to Cultured Corneal Cells

Immortalized human corneal epithelial cells (HCLEs; provided by Dr. Ilene Gipson), and human corneal stromal fibroblasts were cultured as previously described using 8-well coverglass chamber slides (Fisher Scientific, #155409). Cells were incubated with 15 µl (7 µg protein) CFSE-labeled EVs in 0.2 ml serum-free medium for 4 or 16 hours at 37°C. Cells were fixed in 3% paraformaldehyde in PBS for 20 minutes and imaged using an Olympus DP80 fluorescence microscope. For transfer of miRNA, HCLE in 24-well plates were incubated with 8 µg (protein) EVs loaded with miR159a in 20 µl for 10 minutes, then incubation was continued in 0.2 ml Keratinocyte Serum-Free Growth Medium, Thermo Fisher medium for 2, 4, 8, 16, and 24 hours time points. After incubation, cells were released with recombinant trypsin + EDTA (TrypLe) and rinsed by centrifugation in PBS to remove surface-attached EVs. RNA was

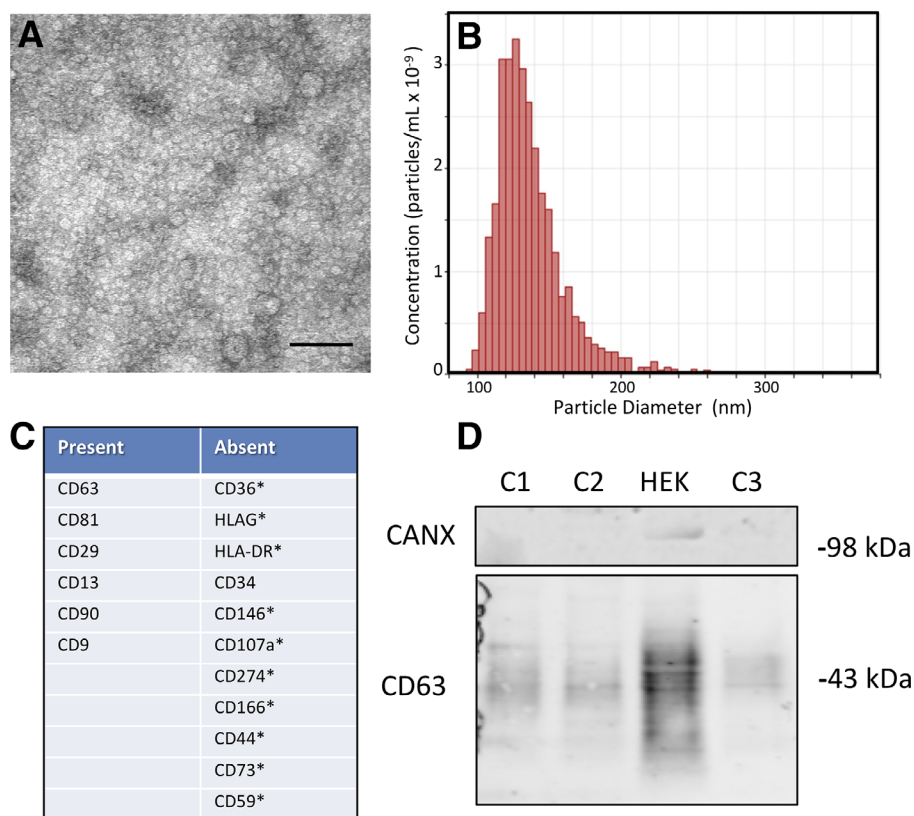


**Figure 1.** CSSC cells secrete extracellular vesicles (EVs). **(A):** Negative staining transmission electron microscopy of a high-speed pellet from conditioned media of cultured CSSC cells shows abundant vesicles with a range of diameters from 16 to 180 nm having a median of 28 nm. **(B):** Size distribution of extracellular vesicles isolated from CSSC conditioned media was examined using resistive pulse sensing as described in the “Materials and Methods” section. **(C):** CD63-bead cytometry was used to identify surface antigens present on the EVs isolated from CSSC. **(D):** Western blotting of 10  $\mu$ g protein from purified EVs from three CSSC cell lines (C1, C2, C3) and from HEK293T cells (HEK). Antibodies to calnexin (CNX) and CD63 were used on the same samples.

isolated and miR159a was detected in cellular RNA by TaqMan qPCR as described below using miR221-3p and miR191-3p as internal controls.

### miRNA Isolation and Analysis

CSSC cells or purified EVs were lysed with RLT buffer, and total RNA, including small RNAs, was isolated using the Qiagen miRNeasy kit according to manufacturer’s directions. miRNA was quantified in samples with Taqman RealTime PCR assays designed for specific miRNAs (Thermo Fisher Scientific, MA). Linearity of the assay was confirmed using dilutions of standard miRNA. Abundance was determined relative to total RNA in the sample as technical triplicates assayed in RNA from three pooled samples. As a control for amplification or losses during the assay process, a nonmammalian miRNA “spike-in” (ath-miR159a) was added to a known concentration to the RNA samples before reverse transcription. miRNA content of CSSC-derived EVs was determined for 800 human miRNA species by screening RNA isolated from EVs produced by CSSC isolated from eight different donors, from human corneal fibroblasts, and from HEK293T cells using a Nanostring Array (Nanostring, Inc., CSO-MIR3-12). Relative abundance was determined using nSolver software. Statistical differences between abundance of miRNA from EVs from three CSSC lines of known regenerative potential from HEK293T EVs was determined using one-sample *t* test.

**RNA sequence analysis.** A strand-specific small RNA library was produced from EV RNA using the QIAseq miRNA library kit (Qiagen) following the manufacturer’s instructions. Postlibrary concentrations were quantified using Qubit Fluorometric Quantification apparatus (Thermo Fisher Scientific, MA). Libraries (2 nM per sample) were sequenced to generate single-end 50 bp reads on a HiSeq 3000 system (Illumina, San Diego, CA). Exosomal small RNA library preparation and sequencing were performed by the UCLA Technology Center for Genomics and Bioinformatics Core. Data were analyzed for human small RNA using the miRBase database [36].

## RESULTS

### EVs from Corneal MSCs

High-speed centrifugation of media conditioned by CSSC produced pellets consisting largely of membrane-enclosed vesicles with apparent diameters of 16–180 nm when examined by negative-stained transmission electron microscopy (Fig. 1A). When these EV particles were purified from conditioned media by repeated sedimentation they showed a size distribution of 120–200 nm (Fig. 1B) using TRPS as described in “Materials and Methods.” Flow cytometric analysis demonstrated several surface proteins previously reported on EVs from stem cells including CD9, CD81, CD29, CD13, CD90 (Fig. 1C, Supporting Information Fig. S2). A number of other proteins previously identified in EVs from cultured cells, however, were not detected

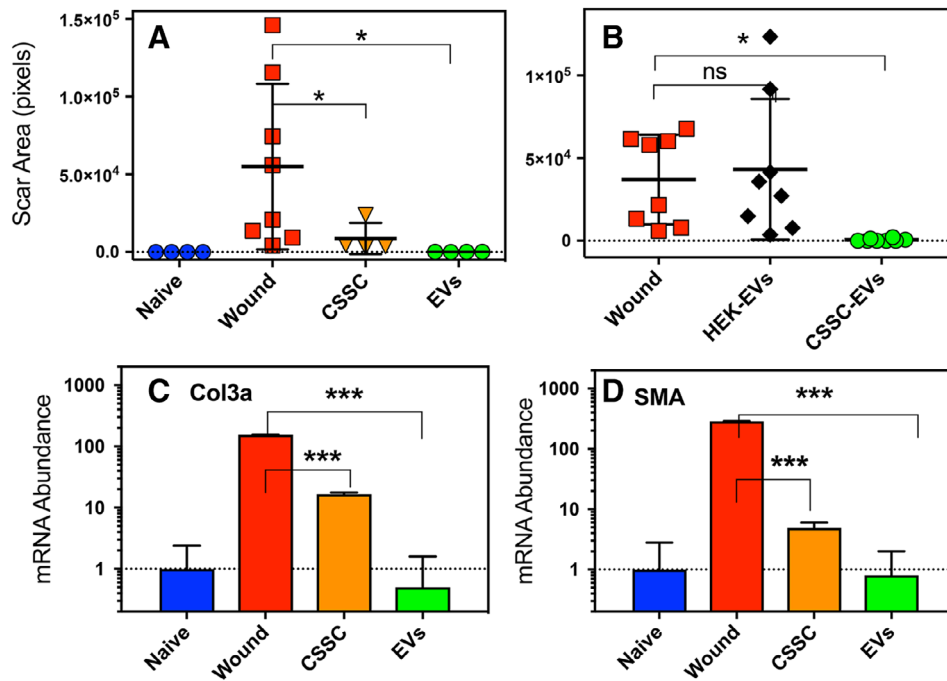


**Figure 2.** EV treatment prevents scar formation after corneal wounding. **(A):** Corneas were wounded by surface debridement and immediately treated with corneal stromal stem cells (CSSC) or with extracellular vesicles (EVs) in a fibrin gel as described in the “Materials and Methods” section. Two weeks after wounding, scar area was assessed by image analysis of the corneas as described in the “Materials and Methods” section. Each point represents scar area of one cornea. **(B):** In a separate experiment, the therapeutic effect of EVs from CSSC and HEK293T cells was compared by measuring scar area. **(C):** Expression of mRNA for collagen 3a1 was compared in corneas from experiment in (A) using qPCR as described in the “Materials and Methods” section. **(D):** Expression of mRNA for smooth muscle actin (SMA, Acta2) was compared using qPCR. Error bars represent standard deviation. In (C) and (D),  $n = 3$ . In (A) and (B),  $n = 8$  (\*,  $p < .05$ ; \*\*\*,  $p < .001$ ) using  $t$  test.

(Fig. 1C) indicating that CSSC EVs display a subset of typical EV surface proteins. Immunoblotting of the EV proteins demonstrated CD63 but not calnexin, a protein present in microvesicles but not in exosomes (Fig. 1D) [37, 38], suggesting that most of the isolated CSSC EVs were products of the endosomal sorting complexes required for transport (ESCRT) endosomal pathway [39].

### Corneal Stromal Stem Cell-Derived EVs Prevent Corneal Scarring In Vivo

Corneas with debridement wounds were treated with CSSC or with CSSC-derived purified EVs in fibrin gel. Visual assessment 2 weeks after wounding found a nearly complete prevention of scarring for both treatments (Fig. 2A, Supporting Information Fig. S3). In a separate experiment, scarring after application of EVs from HEK293T and CSSC were compared. As shown in Figure 2B, the HEK-derived EVs failed to prevent scarring. qPCR was used to analyze expression of RNA for the fibrotic marker collagen 3 (Col3a1) and for myofibroblast marker smooth muscle actin (Acta2), both of which are markedly upregulated 2 weeks after wounding [10, 12]. Both CSSC and CSSC-derived EVs showed a significant inhibition of the upregulation of these genes compared with control wounds (Fig. 2C, 2D).

### Histologic Analysis Shows EVs Treatment Preserves Normal Corneal Morphology

Corneal wounds treated with fibrin gel only continued to demonstrate a pathological tissue morphology for at least a month after wounding. As shown in Figure 3B, vascularization, acellular fibrotic deposits, a reduced number of cuboidal cells in the

basal epithelium, infiltration by leukocytes and areas devoid of keratocytes were evident. Corneas treated with EVs, on the other hand (Fig. 3C) were thinner, showed none of these pathological signs, and were indistinguishable from naïve, unwounded corneas (Fig. 3A).

### CSSC EVs Reduce Early Corneal Infiltration by Neutrophils After Wounding

Our previous studies demonstrated a reduction of corneal infiltration by neutrophil granulocytes resulting from treatment with CSSC after wounding. We assessed neutrophil infiltration at 24 hours after wounding by measurement of corneal myeloperoxidase, an enzyme highly expressed by neutrophils [33]. Based on MPO expression, we found that treatment with CSSC EVs significantly reduced on neutrophil infiltration 24 hours after wounding (Fig. 4A). EVs from HEK293T cells, in contrast, showed no inhibition of neutrophil infiltration (Fig. 4B).

### EVs from CSSC Fuse with Human Corneal Cells and Transfer miRNA

The transfer of miRNA has been suggested as an important functional role for EVs. Analysis of RNA from CSSC EVs using a Nanostring Array showed detectable levels of >200 miRNAs in preparations of EV from CSSC from four different donors (Supporting Information Table S1). To assess the ability of EVs to fuse with corneal cells, cultured human corneal fibroblasts and HCLEs were incubated with fluorescently labeled EV. As shown in Figure 5, within 4 hours, EV had entered both cell types and had assumed a perinuclear localization. Transfer of miRNA was detected by loading the EVs with a synthetic

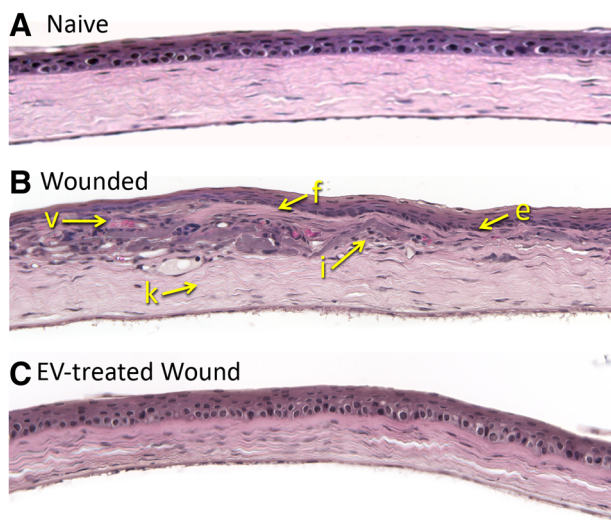


**Figure 3.** Histology of corneal wounds after 1 month. **(A):** H&E staining of a nonwounded (naïve) mouse cornea. **(B):** Cornea with a debridement wound after 4 weeks of healing stained by hematoxylin and eosin shows typical pathology: V, vascularization; f, acellular fibrotic deposits; e, lack of cuboidal cells in epithelial basal layer; i, infiltrate of immune cells; k, areas devoid of keratocytes. **(C):** Typical cornea wounded as in (B) but treated with CSSC EVs shows none of the pathological features associated with scarring. The wounded area in (B) and (C) extends across the full width of tissue shown. Scalebar = 200  $\mu$ m.

miRNA, ath-miR159a, a molecule not present in mammalian cells. A time course of incubation of these loaded EVs with HCLE cells (Fig. 5G), revealed a rapid transfer of this miRNA to the cells, with peak concentration at 4 hours of incubation.

#### miRNA Packaging into EVs Requires Alix Protein

The role of EV miRNA in corneal regeneration was explored by producing EVs with reduced miRNA content. Alix protein (also known as PDCD6IP) was shown previously to be involved in packaging miRNA into EVs during their synthesis in multi-vesicular endosomes [40]. We found that Alix protein was effectively reduced by small interfering RNA (siRNA) transfection of CSSC (Fig. 6A). Quantification of Alix-protein knockdown demonstrated a reduction of 90% compared with scrambled siRNA transfected cells (Fig. 6B).

In cells with Alix knocked down, levels of four miRNAs were not significantly different than those in the control cells (Fig. 6C). However, in EVs secreted by the CSSC with knockdown of Alix, miRNAs were reduced by approximately 85% compared with EVs from control cells (Fig. 6C).

#### Alix Knockdown Eliminates Regenerative Functions of CSSC and CSSC EVs

CSSC with Alix knockdown produced EVs with particle number and protein content similar to CSSC treated with scrambled control siRNA. When healing of corneal wounds was compared after treatment with EVs from control and Alix-KD CSSC, scarring assessed after 14 days revealed a reduced ability to prevent scarring in the EVs containing reduced amounts of miRNA (Fig. 7A). qPCR analysis of the healing corneas found that the upregulation of *Col3a1* and *Acta2* genes in the wounded corneas was not suppressed by EVs with reduced miRNA, whereas EV from control cells completely suppressed upregulation of

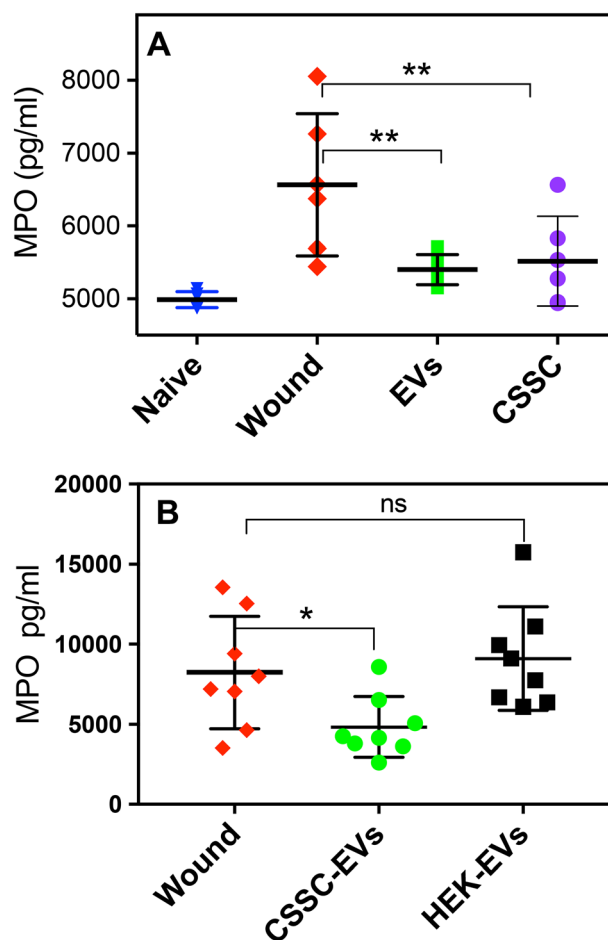


**Figure 4.** EVs suppress neutrophil infiltration. Corneas were wounded by debridement and treated with extracellular vesicles (EVs) or with CSSC. After 24 hours, individual corneas were excised, extracted, and the level of myeloperoxidase (MPO) was measured as described in the “Materials and Methods” section. **(A):** EVs (green) and CSSC (purple) both suppressed MPO activity compared with untreated wounds (red; \*\*,  $p < .01$ ). **(B):** In a separate experiment, EVs from CSSC cells (CSSC-EVs, green) were compared with EVs from HEK273T cells (HEK-Es, gray). Only CSSC-Exo significantly suppressed MPO (\*,  $p < .05$ ).

these mRNAs. Interestingly, treatment of healing wounds with live CSSC cells exhibited a very similar pattern to that of the EVs. Alix knockdown reduced the ability of the cells to prevent scarring and prevented suppression of fibrotic marker genes.

In addition to the expression of fibrotic genes 2 weeks after wounding, expression of early inflammatory genes was suppressed by EVs at 3 days after wounding (Supporting Information Fig. S4). *Chi3l1* [41] and *Lcn2* [42] are both highly expressed in neutrophils. *Adgre (F4/80)* is considered a monocyte/macrophage marker [43] as is *CD80 (B7-1)* [44]. *uPAR* is a protein localized on surface of platelets [45] and *Cxcl-7 (PBP)* is a platelet chemokine protein that attracts neutrophils [46]. *Cxcl-5* is a chemokine expressed by corneal epithelial cells that also attract neutrophils [47]. Expression of each of these genes is markedly upregulated 1–3 days after wounding but is suppressed by EV treatment at the time of wounding. EVs with reduced miRNA content, however, did not suppress the upregulation (Supporting Information Fig. S4).

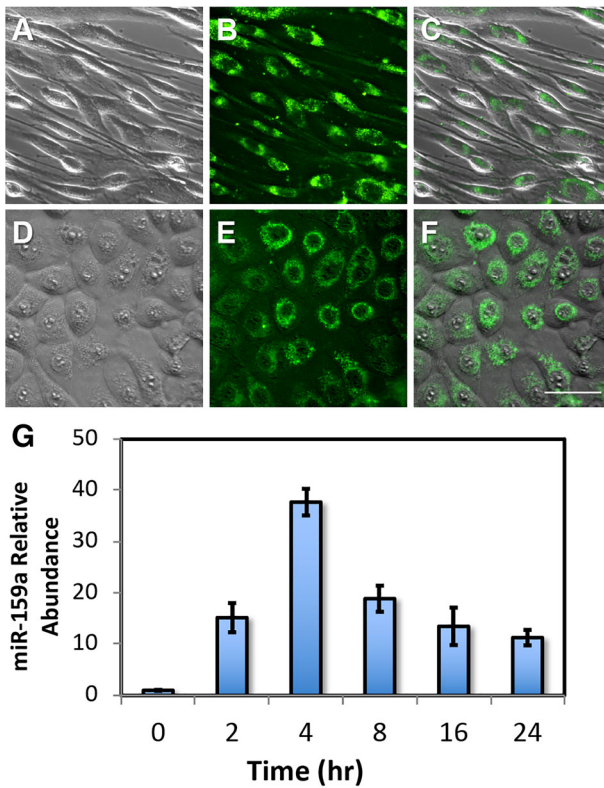


**Figure 5.** Extracellular vesicles (EVs) from CSSC fuse with and transfer microRNA into corneal cells. **(A–F):** EVs, labeled with fluorescent dye carboxyfluorescein succinimidyl ester (CFSE) as described in the “Materials and Methods” section, were transferred to cultures of corneal fibroblasts (A–C) and human corneal epithelial cells (HCLE), (D–F) for 4 hours. The cells were photographed with phase contrast optics (A, D), and fluorescence (B, E). The two images are overlaid in (C) and (F). The scale bar in (F) shows 20  $\mu$ m. **(G):** CFSE labeled EVs loaded with microRNA ath-miR-159a, as described in the “Materials and Methods” section, were transferred to cultures of HCLE cells for the times shown. Cells were rinsed, trypsin-treated to remove extracellular miRNA, and then cellular RNA was assayed for the abundance of ath-miR-159a using qPCR as described in the “Materials and Methods” section.

## DISCUSSION

In the current study, we observed that the regenerative properties of CSSC could be replicated by EVs from those cells. This includes the suppression of visible scars after corneal wounding, suppression of expression of fibrotic genes in wounded corneas, suppression of neutrophil infiltration based on indirect measurement by MPO activity and suppression of expression of inflammatory mRNA 3 days after wounding. Histologic evaluation of the corneas 1 month after corneal wounding showed a normal morphology in EV-treated corneas, whereas untreated wounds demonstrated severe and long-lasting pathologic changes in tissue morphology. Controls with EVs isolated from HEK293T cells showed none of the regenerative properties of CSSC-derived EVs, implicating the unique nature of EVs isolated from CSSC. Flow cytometric comparison of cell surface markers demonstrated few qualitative differences compared with HEK293T cells, but the CSSC EVs lacked some cell surface proteins described as markers for bone marrow and adipose derived MSCs, including CD73, suggesting that surface markers of EV may be dependent on the tissue

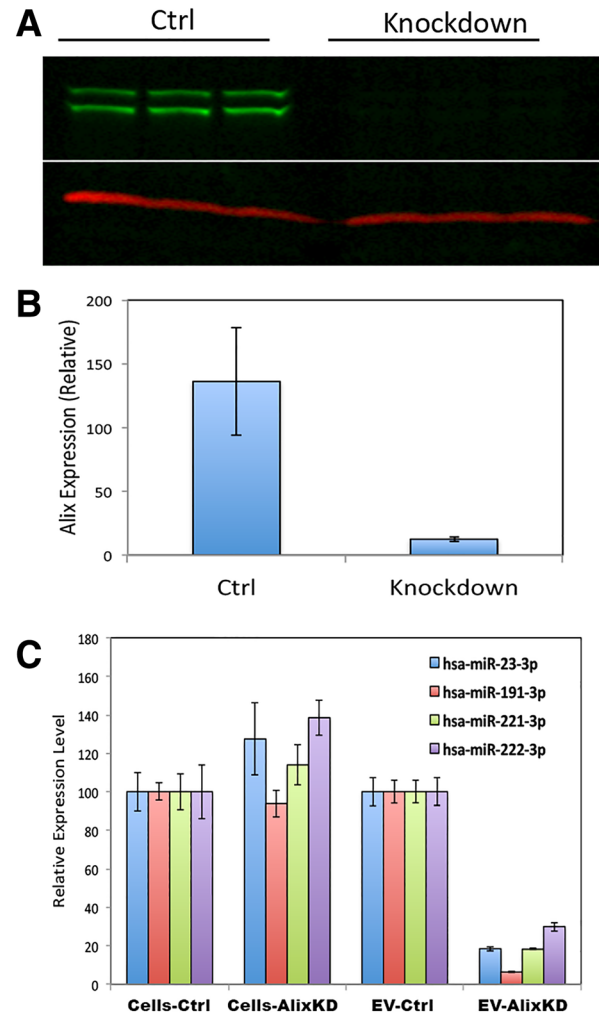


**Figure 6.** Knockdown of Alix protein blocks packaging of miRNA in extracellular vesicles (EVs). CSSC were transfected with siRNA targeting miRNA for Alix protein (knockdown) or with a scrambled control siRNA (Ctrl). **(A):** After 2 days of culture to collect media for EV, cell lysates were subjected to Western blotting for Alix protein (green) and cyclophilin (red) on the same blot. **(B):** Alix expression was quantified using Fiji software. Error bars represent SD of triplicate analyses of Alix protein normalized to cyclophilin in three different lanes. Expression difference was significant ( $p < .05$ ,  $t$  test). **(C):** Four miRNA species were quantified using qPCR in small RNA from CSSC cells transfected with scrambled siRNA (cells-Ctrl) and with Alix siRNA (cells-AlixKD). Technical triplicate analyses found no significant differences in concentration of the four miRNAs comparing each in cells with or without Alix knockdown. The same miRNAs were quantified in EVs isolated from the transfected cells, EV-Ctrl, and EV-AlixKD. The abundance of miRNAs in EVs from AlixKD, was 10%–15% of amount present in EVs from control cells ( $n = 3$ ;  $p < .05$ ).

source of the stem cells. Whether any of these markers influence the regenerative properties of EVs will need to be investigated in further studies.

Biologically, EVs from cultured cells arise from different pathways. Microvesicles are formed by budding of the plasma membrane and exhibit a large range of sizes, whereas exosomes form in intraluminal vesicles inside multivesicular endosomes (MVEs). By fusion of these MVEs with the plasma membrane, these vesicles are released to the extracellular space and thereby known as exosomes. Exosomes are

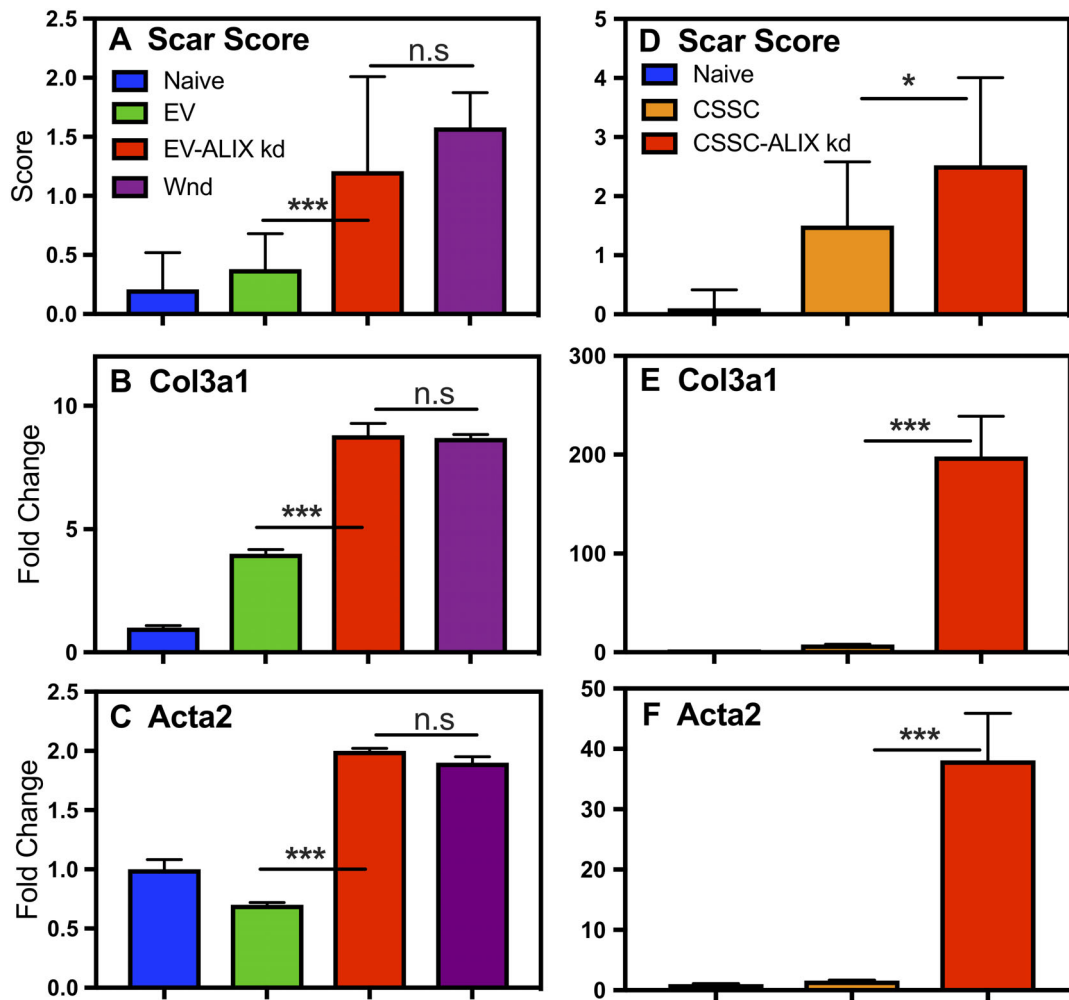


**Figure 7.** Alix knockdown eliminates the regenerative functions of extracellular vesicles (EVs) and CSSC cells. Scarring was assessed 14 days after wounding according to visual scoring of the wounded eyes (**A, D**) and using qPCR to assess mRNA expression of fibrotic genes collagen 3a1 (**B, E**) smooth muscle actin (**C, F**) in nonwounded corneas (naïve, blue), wounded corneas (wound, purple) and wounds treated with CSSC EVs (**A–C**, green) or EVs isolated from CSSC treated with siRNA against Alix (**A–C**, red). The effectiveness of CSSC (**D–F**, orange) and CSSC treated with Alix siRNA (**D–F**, red) was also compared. Scar score (**A, D**) was based on  $n = 8$ . PCR was based on  $n = 3$ .  $p$  values were determined using  $t$  test (\*,  $p < .05$ ; \*\*,  $p < .01$ ; \*\*\*,  $p < .001$ ).

generated in a stepwise fashion controlled by the ESCRT machinery acting as a driver of membrane shaping and scission in the late endosomal membrane. One particular ESCRT-protein, Alix, has been shown to be required for miRNA transfer into exosomal EVs [40]. The knockdown of Alix in CSSC in our experiment resulted in an 85% reduction of miRNA content in EVs without reducing the number of particles or EV protein content significantly (Fig. 6). The ability to generate EVs lacking miRNA allowed us to test the role of the miRNA in the regenerative function of these vesicles.

In vitro, CSSC-derived EVs rapidly fused with corneal fibroblasts and corneal epithelial cells and delivered miRNA to these cells. Moreover, when miRNA abundance in the CSSC EVs was reduced by Alix knockdown, the regenerative function of the EVs was eliminated. Wounded corneas treated with EVs lacking miRNA developed visible scarring and expressed genes associated with fibrosis and inflammatory cell infiltration, compared with wounds treated with control CSSC-derived EVs. These results suggest a role for miRNA in the anti-inflammatory/regenerative function displayed by the CSSC EVs. Such a

function is consistent with a number of recent studies that have linked miRNA delivery by EVs to regenerative, antifibrotic, and immune suppressive properties of the vesicles [48–57]. Some authors have suggested that the small amount of miRNA in EVs makes it more likely that a protein cargo is involved in their biological properties [58]. Others have suggested the low level of miRNA might be counteracted by selective delivery of miRNA to targeted cell populations such as macrophages or that nonstoichiometric action of miRNAs may occur via binding of the RNA to cell receptors [59]. Our calculations, based on RNA content and the observation that miRNAs make up to 7% of the RNA content of the EV nucleic acid (Supporting Information Fig. S5) suggest that each mouse cornea received 100–200 fmole of miRNA. The more abundant miRNAs (shown in Supporting Information Table S1) would therefore have been delivered in low fmole levels. Whether this amount represents enough of any one species of miRNA to effect the biological function we observed will need to be tested in further experiments using synthetic individual miRNAs.



Corneal scarring is the cause of blindness for millions of individuals, especially in developing countries [60, 61]. The current standard of care is corneal transplantation to replace the scarred corneal tissue. This procedure has good results, but requires ongoing medical care. Typically a graft has a half-life of only 10 years. More importantly, it is estimated that only one individual in 70 with corneal visual impairment has access to donated tissue for a transplant [62]. Clinical trials using CSSC (NCT02948023) to treat corneal scarring were recently completed in Hyderabad, India and are expected to be approved for clinical use. This approach can circumvent the requirement for donated corneal tissue and a full thickness graft for many individuals with corneal scarring. The cell-based therapy links treatment to a large medical center that can provide fresh preparations of CSSC stem cells for each procedure. Our work predicts that the use of CSSC EVs or of a reagent capable of delivering the miRNA component of those EVs could provide a reagent that is more stable, transportable, and cheaper than live cells. Development of such a reagent might encounter reduced regulatory hurdles compared with live cells and could open the prospect of improved vision for a greatly increased number of affected individuals. Our current study provides new information as to the mechanism by which MSCs induce tissue regeneration and at the same time points the way toward a potentially highly effective form of new therapy.

Understanding the properties of EVs required for clinical efficacy including the role of miRNA and protein content will provide an avenue for an EV-based therapy for corneal scarring and potentially serve as a model for use of EVs in other clinical applications.

## CONCLUSION

MSCs isolated from cornea restore transparency to scarred corneas and are currently in clinical trials to regress existing human cornea scars. As with other MSC, CSSC isolated from different donors vary in their regenerative potency. Understanding of the molecular mechanism of this process can lead to improved consistency and potency of cellular reagents as well as the development of manufactured reagents that do

not rely on use of living cells, thus improving efficacy, safety, and cost of the therapy. Our finding that EVs can accomplish cornea regeneration without the need for live cells represents significant progress toward these goals.

## ACKNOWLEDGMENTS

We appreciate the skilled assistance of Katherine Davoli HTL(ASCP)CM in preparing the histology slides of wounded corneas and of Kira Lathrop in help with microscopy. This work was supported by NIH EY016415 (J.L.F.), NIH P30 EY008098, Eye and Ear Foundation of Pittsburgh, Stein Innovator Award from Research to Prevent Blindness (J.L.F.), Department of Defense W81WH-14-1-0465 (J.L.F.), NEI R01 EY028557 (S.X.D.), NEI R01 EY021797 (S.X.D.), CLIN1-08686 California Institute for Regenerative Medicine (S.X.D.).

## AUTHOR CONTRIBUTIONS

G.S., I.K.: conception and design, collection and/or assembly of data, data analysis and interpretation, manuscript writing, final approval of manuscript; M.L.F.: collection and/or assembly of data, data analysis and interpretation, manuscript writing, administrative support, final approval of manuscript; M.M.M., D.B.S., M.G.: collection and/or assembly of data; R.D., A.D.S., S.X.D.: collection and/or assembly of data, data analysis and interpretation; J.L.F.: conception and design, financial support, collection and/or assembly of data, data analysis and interpretation, manuscript writing, final approval of manuscript.

## DISCLOSURE OF POTENTIAL CONFLICTS OF INTEREST

The authors indicated no potential conflicts of interest.

## DATA AVAILABILITY STATEMENT

The data that support the findings of this study are available from the corresponding author upon reasonable request.

## REFERENCES

- Shafei AE, Ali MA, Ghanem HG et al. Mesenchymal stem cell therapy: A promising cell-based therapy for treatment of myocardial infarction. *J Gene Med* 2017;19. <https://doi.org/10.1002/jgm.2995>
- Du Y, Funderburgh ML, Mann MM et al. Multipotent stem cells in human corneal stroma. *STEM CELLS* 2005;23:1266–1275.
- Funderburgh ML, Du Y, Mann MM et al. PAX6 expression identifies progenitor cells for corneal keratocytes. *FASEB J* 2005;19:1371–1373.
- Du Y, Sundarraj N, Funderburgh ML et al. Secretion and organization of a cornea-like tissue in vitro by stem cells from human corneal stroma. *Invest Ophthalmol Vis Sci* 2007;48:5038–5045.
- Pinnamaneni N, Funderburgh JL. Concise review: Stem cells in the corneal stroma. *STEM CELLS* 2012;30:1059–1063.
- Wu J, Du Y, Mann MM et al. Bioengineering organized, multilamellar human corneal stromal tissue by growth factor supplementation on highly aligned synthetic substrates. *Tissue Eng Part A* 2013;19:2063–2075.
- Hertsenberg AJ, Funderburgh JL. Stem cells in the cornea. *Prog Mol Biol Transl Sci* 2015;134:25–41.
- Funderburgh JL, Funderburgh ML, Du Y. Stem cells in the limbal stroma. *Ocul Surf* 2016;14:113–120.
- Syed-Picard FN, Du Y, Hertsenberg AJ et al. Scaffold-free tissue engineering of functional corneal stromal tissue. *J Tissue Eng Regen Med* 2018;12:59–69.
- Basu S, Hertsenberg AJ, Funderburgh ML et al. Human limbal biopsy-derived stromal stem cells prevent corneal scarring. *Sci Transl Med* 2014;6:266ra172.
- Shojaati G, Khandaker I, Sylakowski K et al. Compressed collagen enhances stem cell therapy for corneal scarring. *STEM CELLS TRANSLATIONAL MEDICINE* 2018;7:487–494.
- Du Y, Carlson EC, Funderburgh ML et al. Stem cell therapy restores transparency to defective murine corneas. *STEM CELLS* 2009;27:1635–1642.
- Caplan AI, Sorrell JM. The MSC curtain that stops the immune system. *Immunol Lett* 2015;168:136–139.
- Spees JL, Lee RH, Gregory CA. Mechanisms of mesenchymal stem/stromal cell function. *Stem Cell Res Ther* 2016;7:125.
- Wang M, Yuan Q, Xie L. Mesenchymal stem cell-based immunomodulation: Properties and clinical application. *Stem Cells Int* 2018;2018:3057624.
- Toh WS, Zhang B, Lai RC et al. Immune regulatory targets of mesenchymal stromal cell exosomes/small extracellular vesicles in tissue regeneration. *Cytotherapy* 2018;20:1419–1426.
- Lai TS, Wang ZH, Cai SX. Mesenchymal stem cell attenuates neutrophil-predominant

inflammation and acute lung injury in an in vivo rat model of ventilator-induced lung injury. *Chin Med J* 2015;128:361–367.

18 Jiang D, Muschhammer J, Qi Y et al. Suppression of neutrophil-mediated tissue damage—A novel skill of mesenchymal stem cells. *STEM CELLS* 2016;34:2393–2406.

19 Li H, Rong P, Ma X et al. Paracrine effect of mesenchymal stem cell as a novel therapeutic strategy for diabetic nephropathy. *Life Sci* 2018;215:113–118.

20 Phinney DG, Pittenger MF. Concise review: MSC-derived exosomes for cell-free therapy. *STEM CELLS* 2017;35:851–858.

21 Safari S, Malekvandfar F, Babashah S et al. Mesenchymal stem cell-derived exosomes: A novel potential therapeutic avenue for cardiac regeneration. *Cell Mol Biol (Noisy-le-Grand)* 2016;62:66–73.

22 Suzuki E, Fujita D, Takahashi M et al. Therapeutic effects of mesenchymal stem cell-derived exosomes in cardiovascular disease. *Adv Exp Med Biol* 2017;998:179–185.

23 Wu P, Zhang B, Shi H et al. MSC-exosome: A novel cell-free therapy for cutaneous regeneration. *Cytotherapy* 2018;20:291–301.

24 Qing L, Chen H, Tang J et al. Exosomes and their microRNA cargo: New players in peripheral nerve regeneration. *Neurorehabil Neural Repair* 2018;32:765–776.

25 Park K. Exosome-based therapeutic approach for muscle regeneration. *J Control Release* 2016;222:176.

26 Bollini S, Smits AM, Balbi C et al. Triggering endogenous cardiac repair and regeneration via extracellular vesicle-mediated communication. *Front Physiol* 2018;9:1497.

27 Zhang S, Chuah SJ, Lai RC et al. MSC exosomes mediate cartilage repair by enhancing proliferation, attenuating apoptosis and modulating immune reactivity. *Biomaterials* 2018;156:16–27.

28 Cunnane EM, Weinbaum JS, O'Brien FJ et al. Future perspectives on the role of stem cells and extracellular vesicles in vascular tissue regeneration. *Front Cardiovasc Med* 2018;5:86.

29 Behera J, Tyagi N. Exosomes: Mediators of bone diseases, protection, and therapeutics potential. *Oncoscience* 2018;5:181–195.

30 Nakamura Y, Miyaki S, Ishitobi H et al. Mesenchymal-stem-cell-derived exosomes accelerate skeletal muscle regeneration. *FEBS Lett* 2015;589:1257–1265.

31 Mead B, Tomarev S. Bone marrow-derived mesenchymal stem cells-derived exosomes promote survival of retinal ganglion cells through miRNA-dependent mechanisms. *STEM CELLS TRANSLATIONAL MEDICINE* 2017;6:1273–1285.

32 Boote C, Du Y, Morgan S et al. Quantitative assessment of ultrastructure and light scatter in mouse corneal debridement wounds. *Invest Ophthalmol Vis Sci* 2012;53:2786–2795.

33 Hertszenberg AJ, Shojaati G, Funderburgh ML et al. Corneal stromal stem cells reduce corneal scarring by mediating

neutrophil infiltration after wounding. *PLoS One* 2017;12:e0171712.

34 Théry C, Witwer KW, Aikawa E et al. Minimal information for studies of extracellular vesicles 2018 (MISEV2018): A position statement of the International Society for Extracellular Vesicles and update of the MISEV2014 guidelines. *J Extracell Vesic* 2018;7:1535750.

35 Zhang D, Lee H, Zhu Z et al. Enrichment of selective miRNAs in exosomes and delivery of exosomal miRNAs in vitro and in vivo. *Am J Physiol Lung Cell Mol Physiol* 2017;312:L110–L121.

36 Fehlmann T, Backes C, Kahraman M et al. Web-based NGS data analysis using miRMaster: A large-scale meta-analysis of human miRNAs. *Nucleic Acids Res* 2017;45:8731–8744.

37 Haraszti RA, Didiot MC, Sapp E et al. High-resolution proteomic and lipidomic analysis of exosomes and microvesicles from different cell sources. *J Extracell Vesic* 2016;5:32570.

38 Mears R, Craven RA, Hanrahan S et al. Proteomic analysis of melanoma-derived exosomes by two-dimensional polyacrylamide gel electrophoresis and mass spectrometry. *Proteomics* 2004;4:4019–4031.

39 Cocucci E, Meldolesi J. Ectosomes and exosomes: Shedding the confusion between extracellular vesicles. *Trends Cell Biol* 2015;25:364–372.

40 Iavello A, Frech VS, Gai C et al. Role of Alix in miRNA packaging during extracellular vesicle biogenesis. *Int J Mol Med* 2016;37:958–966.

41 Volck B, Price PA, Johansen JS et al. YKL-40, a mammalian member of the chitinase family, is a matrix protein of specific granules in human neutrophils. *Proc Assoc Am Physicians* 1998;110:351–360.

42 Venge P. Human neutrophil lipocalin (HNL) as a biomarker of acute infections. *Ups J Med Sci* 2018;123:1–8.

43 Gordon S, Hamann J, Lin HH et al. F4/80 and the related adhesion-GPCRs. *Eur J Immunol* 2011;41:2472–2476.

44 Chen B, Ni Y, Liu J et al. Bone marrow-derived mesenchymal stem cells exert diverse effects on different macrophage subsets. *Stem Cells Int* 2018;2018:1–9.

45 Piguat PF, Vesin C, Donati Y et al. Urokinase receptor (uPAR, CD87) is a platelet receptor important for kinetics and TNF-induced endothelial adhesion in mice. *Circulation* 1999;99:3315–3321.

46 Rajarathnam K, Schnoor M, Richardson RM et al. How do chemokines navigate neutrophils to the target site: Dissecting the structural mechanisms and signaling pathways. *Cell Signal* 2019;54:69–80.

47 Sun Y, Fox T, Adhikary G et al. Inhibition of corneal inflammation by liposomal delivery of short-chain, C-6 ceramide. *J Leukoc Biol* 2008;83:1512–1521.

48 He J, Wang Y, Lu X et al. Micro-vesicles derived from bone marrow stem cells protect the kidney both in vivo and in vitro by

microRNA-dependent repairing. *Nephrology (Carlton)* 2015;20:591–600.

49 Fang S, Xu C, Zhang Y et al. Umbilical cord-derived mesenchymal stem cell-derived exosomal microRNAs suppress myofibroblast differentiation by inhibiting the transforming growth factor-beta/SMAD2 pathway during wound healing. *STEM CELLS TRANSLATIONAL MEDICINE* 2016;5:1425–1439.

50 Qu Y, Zhang Q, Cai X et al. Exosomes derived from miR-181-5p-modified adipose-derived mesenchymal stem cells prevent liver fibrosis via autophagy activation. *J Cell Mol Med* 2017;21:2491–2502.

51 Fernandez-Messina L, Gutierrez-Vazquez C, Rivas-García E et al. Immunomodulatory role of microRNAs transferred by extracellular vesicles. *Biol Cell* 2015;107:61–77.

52 Graner MW, Schnell S, Olin MR. Tumor-derived exosomes, microRNAs, and cancer immune suppression. *Semin Immunopathol* 2018;40:505–515.

53 Chen TS, Lai RC, Lee MM et al. Mesenchymal stem cell secretes microparticles enriched in pre-microRNAs. *Nucleic Acids Res* 2010;38:215–224.

54 Zhang S, Teo KYW, Chuah SJ et al. MSC exosomes alleviate temporomandibular joint osteoarthritis by attenuating inflammation and restoring matrix homeostasis. *Biomaterials* 2019;200:35–47.

55 Zhang D, Lee H, Wang X et al. Exosome-mediated small RNA delivery: A novel therapeutic approach for inflammatory lung responses. *Mol Ther* 2018;26:2119–2130.

56 Ma T, Chen Y, Chen Y et al. MicroRNA-132, delivered by mesenchymal stem cell-derived exosomes, promote angiogenesis in myocardial infarction. *Stem Cells Int* 2018;2018:3290372.

57 Ding Y, Cao F, Sun H et al. Exosomes derived from human umbilical cord mesenchymal stromal cells deliver exogenous miR-145-5p to inhibit pancreatic ductal adenocarcinoma progression. *Cancer Lett* 2018;442:351–361.

58 Toh WS, Lai RC, Zhang B et al. MSC exosome works through a protein-based mechanism of action. *Biochem Soc Trans* 2018;46:843–853.

59 Chevillet JR, Kang Q, Ruf IK et al. Quantitative and stoichiometric analysis of the microRNA content of exosomes. *Proc Natl Acad Sci USA* 2014;111:14888–14893.

60 Flaxman SR, Bourne RRA, Resnikoff S et al. Global causes of blindness and distance vision impairment 1990–2020: A systematic review and meta-analysis. *Lancet Glob Health* 2017;5:e1221–e1234.

61 Wong KH, Kam KW, Chen LJ et al. Corneal blindness and current major treatment concern-graft scarcity. *Int J Ophthalmol* 2017;10:1154–1162.

62 Gain P, Jullienne R, He Z et al. Global survey of corneal transplantation and eye banking. *JAMA Ophthalmol* 2016;134:167–173.



See [www.StemCellsTM.com](http://www.StemCellsTM.com) for supporting information available online.